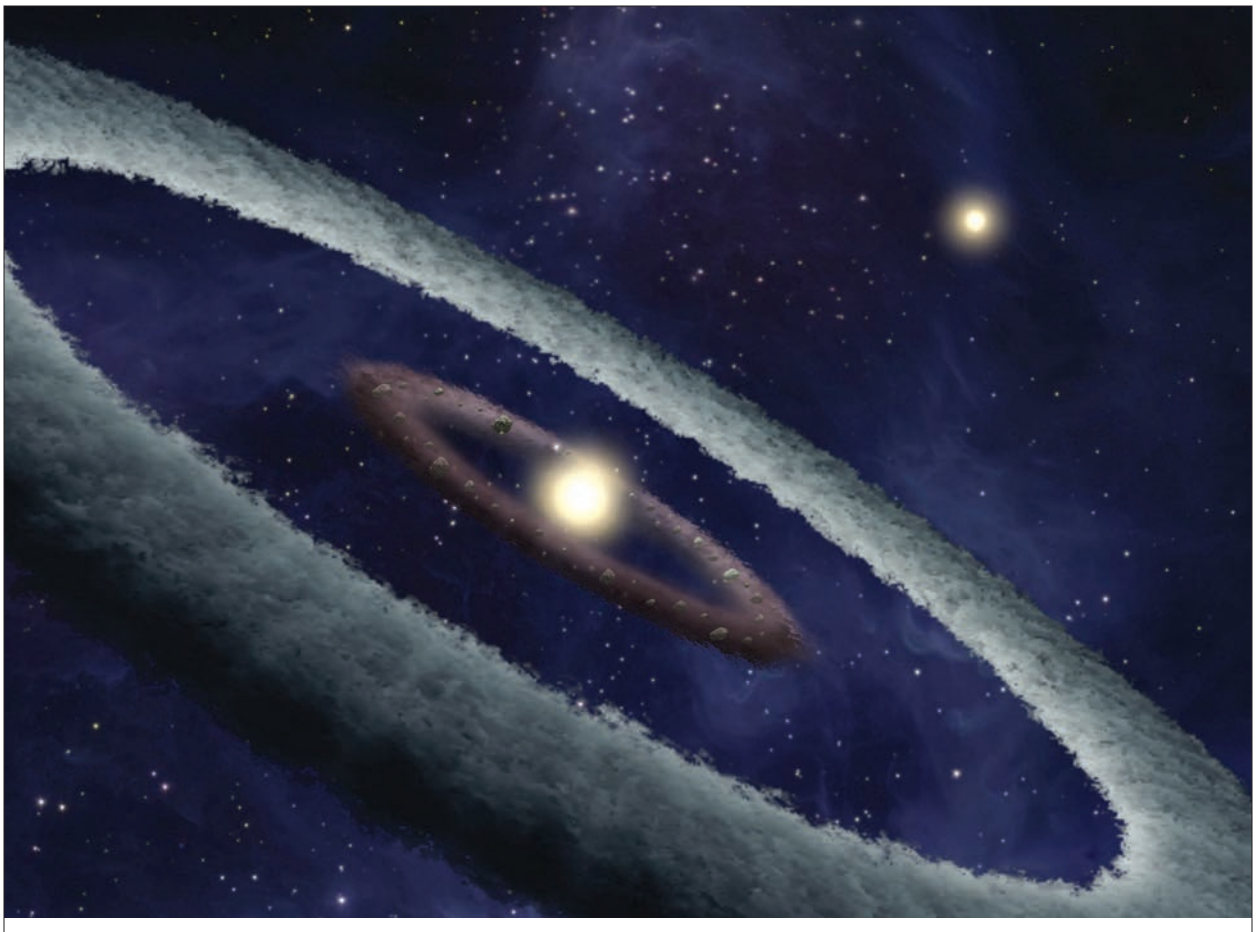

Research Journal of Physics

ISSN 1819-3463

Academic Journals Inc.

www.academicjournals.com

Research Journal of Physics 6 (1): 1-18, 2012
ISSN 1819-3463 / DOI: 10.3923/rjp.2012.1.18

Seismic Refraction Prospecting for Groundwater: A Case Study of Golden Heritage Estate, Ogun State

[1]L. Adeoti, [2]O.M. Alile, [3]O. Uchegbulam and [4]R.B. Adegbola
[1]Department of Geosciences, University of Lagos, Akoka, Lagos, Nigeria
[2]Department of Physics, Covenant University, Ota, Ogun State, Nigeria
[3]Department of Physics and Energy Studies, Western Delta University, Oghara, Delta State, Nigeria
[4]Department of Physics, Lagos State University, Ojo, Lagos

Corresponding Author: O.M. Alile, Department of Physics, Covenant University, Ota, Ogun State, Nigeria

ABSTRACT

The seismic refraction investigation was carried out using the seismograph and it involved twenty-two profiles spread over three traverses with 24 spreads per profile along the major path that passes through the Golden Heritage Estate. A distance of 72 m per profile was utilized for seismic refraction survey. The result shows that the seismic refraction layers delineated were three and first one have an average velocity of 736 m sec^{-1} and thickness of 2-6 m, indicating topsoil. Seismic layer 2 on its part has an average velocity of 1468.18 m sec^{-1} and thickness 3-8 m, indicating laterite. Then the third seismic layer has an average velocity of 2272.73 m sec^{-1} and thickness of 5-12 m, indicating sand. These layers delineated by seismic refraction are characterized by velocity increase with depth. The sand units in the layers delineated acts as the aquifer units. Also the seismic refraction survey could not image the second, third and subsequent aquifers due to the weaker energy source used, hence, it is suggested that for future studies in order to be able to map deeper horizons, stronger energy source should be used.

Key words: Seismic, refraction survey, underground water, velocity increase, energy source

INTRODUCTION

Generally the Seismic method utilizes the propagation of waves through the earth. This propagation depends upon the elastic properties of the rocks. The size and shape of a solid body can be changed by applying force. The body tends to return to its original condition when the external forces are removed. Similarly, a fluid resists changes in sizes (volume) but not changes in shape. This property of resisting changes in size or shape and of returning to the undeformed condition when the external forces are removed is called elasticity. A perfectly elastic body is one that recovers completely after being deformed. Many substances including rocks can be considered to be perfectly elastic without appreciable error provided the deformations are small. The seismic refraction method is utilized such that the seismograph data obtained help to determine the precise depth to weathered basement and overburden thickness such that the different lithologies within the subsurface can easily be predicted (Tearpock and Bischke, 1991). Therefore, the first arrivals on the seismic signals derived from the seismic refraction method are plotted against shot distances to determine depth information. The study area covers about 1×1 km.

The depth to water table in unconsolidated aquifers using the seismic refraction has been done (Haeni, 1986). The shape of bedrock surface and determination of the thickness of saturated

aquifer has been worked on using seismic refraction method (Lennox and Carlson, 1967; Watts *et al*., 1975). Ackermann *et al*. (1986) used the seismic refraction method for hydrological studies in deep alluvial basin. The seafloor was surveyed using shallow seismic refraction method (Hunter and Pullan, 1990). Groundwater exploration in Sudan sub-Saharan Africa was carried out using the same seismic refraction method (Van Overmeeren, 1981). Seismic refraction survey method employs seismic energy which bounces back to the surface after traveling through the ground along refracted ray paths (Philip, 2001). Such that the first arrival of seismic energy at a detector source offset from a seismic source always represents either a direct or refracted ray. Here, attention is concentrated on first arrival (or onset) of the seismic energy.

Then the time-distance plots of the first arrivals are interpreted to derive information on the depth to refracting interfaces, these are also called Refractors which separate layers of different seismic velocity. Reflection seismograms may contain reflection events as subsequent arrivals, this gives rise to relatively high reflection coefficients which are associated with incident rays on an interface at angles near the critical angle leading to strong wide angle reflection commonly detected at the greater recording ranges that characterize large scale refraction surveys.

Geology of study area: The first major transgression in South-west Nigeria occurred during the Maastrichtian which gave rise to sediments of the Abeokuta formation deposited as the oldest formation in the study area. This formation is mainly composed of poorly sorted ferruginized grit, siltstone and mudstone with shale-clay layers (Kogbe, 1989). The Abeokuta formation has its lateral equivalence in the east as the Nsukka formation. The formation is partly marine, brackish and freshwater in origin; it thickens and then continues into Dahomey. This is overlain by the Ewekoro formation and then the Akinbo formation both of which are of the Paleocene age (Adegoke *et al*., 1970) and they have their equivalence in the east as the Imo formation. The type section of the Ewekoro formation is the limestone which is exposed in the quarry at Ewekoro.

Akinbo formation on its part is the upper beds of shale that overlies the limestone and this could be of the lowermost Eocene age. They were however, accorded formational status as the shale overlying the Ewekoro limestone (Ogbe, 1970). The top of the formation is marked by pure grey gritty sand and then little clay. This then passes gradationally into massive mud. This is then overlain by the Oshosun formation which is usually marine through out its thickness and of the Eocene age. This is then overlain by a sequence of predominantly coarse sandy estuarine, deltaic and continental beds which display rapid lateral facies changes and it is named the Illaro formation. Both the Oshosun and Illaro formation have their lateral equivalence as Ameki formation in the eastern part of Nigeria. However the Illaro formation has been tentatively assigned a Lutenian age (Slansky, 1962).

In the sandy Abeokuta formation which happens to be the oldest formation in the study area underlain by the basement complex harbours an aquifer zone which can be termed unattractive since it can not be considered as good prospect for ground water exploration because of the impending low yield capactity. However, the Abeokuta formation is overlain by the Ewekoro formation which also bears similar aquifer characteristics and this is further overlain by the Akinbo formation which has been found to be a good source of ground water exploration. The structural features that occur within the basement rocks are due to tectonic activities and they include: joints, faults and fractures. It is the fractures that influence the ground water in crystalline rocks, hence, the water bearing zones consist of weathered materials. Deeply weathered zones occur usually in pockets as they rarely exceed 40 m in depth.

Theories of seismic refraction: In order to proceed analyzing the theories in seismic refraction one should be aware that the subsurface is composed of a series of layers separated by plane and even dipping interfaces. Seismic velocities are also uniform within each layer and layer velocities increase with depth such that ray paths are restricted to vertical plane containing the profile line. The theory of elasticity relates the forces that are applied to the external surfaces of a body to the resulting changes in size and shape. The relation between the applied forces and the deformation are most conveniently expressed in terms of the concepts of stress and strain. In order to calculate the strains when the stresses are known, we must know the relationship between stress and strain. When the strains are small, this relation is given by Hooke's law which states that a given strain is directly proportional to the stress producing it. In general, Hooke's law leads to complicated relations but when the medium is isotropic that is, when properties do not depend upon direction, it can be expressed in the following relatively simple form:

$$\sigma = \lambda\Delta + 2\mu\varepsilon \tag{1a}$$

$$\sigma = \mu\varepsilon \tag{1b}$$

The quantities λ and μ are known as lame's constants. If we write:

$$\varepsilon_{ij} = \left(\sigma_{ij}/\mu\right)$$

It is evident that the smaller ε_{ij} is, the larger μ is for a given σ_{ij}. Therefore, μ is a measure of the resistance to sharing strain and is often referred to as the modulus of rigidity or shear modulus. Although, Hooke's law has wide application, it does not hold for large stresses. Hooke's law no longer holds when the stress is increased beyond the elastic limit.

Lame's constants are convenient when we are using Eq. 1a and b, other elastic constant are also used. These are young modulus (E) Poisson's ratio (σ) and the bulk modulus (k). Let us define E and σ by the relations:

$$E = \sigma_{xx}/\varepsilon_{xx} \tag{2}$$

$$\sigma = \varepsilon_{yy}/\varepsilon_{xx} = -\varepsilon_{zz}/\varepsilon_{xx} \tag{3}$$

The minus is inserted to make σ positive. To define k, we consider a medium subjected only to a hydrostatic pressure p. this is equivalent to the statements:

$$\sigma_{xx} = \sigma_{yy} = \sigma_{zz} = -p \tag{4a}$$

$$\sigma_{xy} = \sigma_{yz} = \sigma_{zz} = 0 \tag{4b}$$

Then k is define as the ratio of the pressure to the dilatation.

Therefore:

$$k = -P/\Delta \tag{4c}$$

The minus sign is to make k positive substituting these values in Hooke's law, we obtain the following relation between E, σ, k and Lame's constant λ and μ.

Therefore:

$$E = \frac{\mu(3\lambda + 2\mu)}{\lambda + \mu} \tag{4d}$$

$$\sigma = \frac{\lambda}{\lambda + \mu} \tag{4e}$$

$$K = \frac{3\lambda + 2\mu}{3} \tag{4f}$$

Rocks, especially sedimentary and metamorphic rocks are frequently not isotropic. Measurement of the elastic constants of sedimentary rock often yields values which depend upon the direction of measurement and difference of 20 to 25% have been reported between measurements parallel and normal to the bedding plane. Inspite of this, in discussing waves propagating, we generally ignore such difference and treat sedimentary rocks as isotopic media, the result are always useful and on the contrary leads to extremely complex and cumbersome mathematical equations. The elastic constants are defined in such a way that they are positive numbers. As a result of this, one must have value between 0 and 0.5. Value range from 0.05 for very hard, rigid rocks to about 0.45 for soft, poorly consolidated materials. Liquids have no resistance to shear and hence for them μ = 0. For most rocks, e, k and μ lie in the range from 0.2 to 1.2 megabars (2×10^{10} to 12×10^{10} N m^{-2}), e is the largest and μ the smallest of the three. Birch (1966), gave an extensive table of elastic constant of rocks. Let us consider what happens when the stresses are not in equilibrium. In wave motion from the Fig. 1, we assume that the stresses on the rear face of the element of volume are as shown but that the stresses on the front face are, respectively:

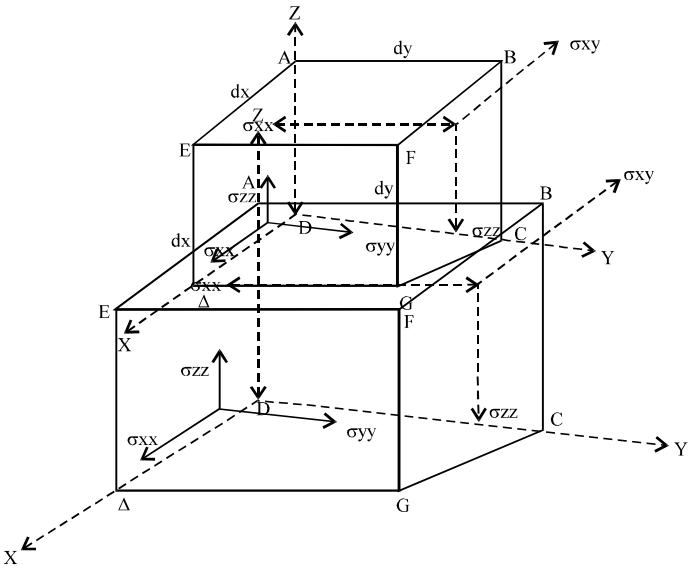

Fig. 1: Components of stress

$$\text{stress} = \sigma_{xx} + \frac{\partial \sigma_{xx}}{\partial x} d_x$$

$$\text{stress} = \sigma_{yx} + \frac{\partial \sigma_{yx}}{\partial x} d_x$$

$$\text{stress} = \sigma_{zx} + \frac{\partial \sigma_{zx}}{\partial_x} d_x$$

Since these stresses are opposite to those acting on the rear face, the net stresses are:

$$\frac{\partial \sigma_{xx}}{\partial x} dx, \frac{\partial \sigma_{yx}}{\partial x} dx, \frac{\partial \sigma_{zx}}{\partial x} dx$$

These stresses act on a face having an area (dydz) and affect the volume (dxdydz), then the value of the net force per unit volume in the direction of the x-,y-,z- axes becomes:

$$\frac{\partial \sigma_{xx}}{\partial x}, \frac{\partial \sigma_{xy}}{\partial x}, \frac{\partial \sigma_{zx}}{\partial x}$$

respectively.

Also, similar expression holds for the other faces. Therefore, the expression for the total force in the direction of the x-axis gives:

$$\left(\frac{\partial \sigma_{xx}}{\partial x} + \frac{\partial \sigma_{xy}}{\partial y} + \frac{\partial \sigma_{xz}}{\partial z} \right)$$

From Newton's second law of motion which states that the unbalanced force equals the product of mass and it's acceleration thus, the equation of motion along the x-axis is:

$$\rho \frac{\partial^2 u}{\partial t^2} = \frac{\partial \sigma_{xx}}{\partial x} + \frac{\partial \sigma_{xy}}{\partial y} + \frac{\partial \sigma_{xz}}{\partial z} \tag{5}$$

Where:

$$\rho \frac{\partial^2 u}{\partial t^2} \Longrightarrow \text{Unbalanced force in the x-direction, } \rho \Longrightarrow \text{density}$$

Similar equation can be written along y- and z-axis.

Equation 5 relates the displacement to the stresses. We can obtain an equation involving only displacement by using Hooke's Law to replace the stresses with strains and then expressing the strains in terms of the displacement using the following equation and Eq. 1a and b:

$$\left.\begin{aligned} \varepsilon_{xx} &= \frac{\partial u}{\partial x} \\ \varepsilon_{xy} &= \frac{\partial u}{\partial y} \\ \varepsilon_{zz} &= \frac{\partial w}{\partial z} \end{aligned}\right\} \Longrightarrow \text{Normal strains, } \left.\begin{aligned} \varepsilon_{xy} = \varepsilon_{yx} &= \frac{\partial v}{\partial x} + \frac{\partial u}{\partial y} \\ \varepsilon_{yz} = \varepsilon_{zy} &= \frac{\partial w}{\partial y} + \frac{\partial v}{\partial z} \\ \varepsilon_{zx} = \varepsilon_{xz} &= \frac{\partial u}{\partial z} + \frac{\partial w}{\partial x} \end{aligned}\right\} \Longrightarrow \text{shearing strains}$$

$$\Delta = \varepsilon_{xx} + \varepsilon_{yy} + \varepsilon_{zz} = \frac{\partial u}{\partial x} + \frac{\partial v}{\partial y} + \frac{\partial w}{\partial z} \text{ ---------- } \Longrightarrow \text{ dilatation } \Longrightarrow \text{ change in volume per unit volume}$$

thus:

$$\begin{aligned}
\rho\frac{\partial^2 u}{\partial t^2} &= \frac{\partial \sigma_{xx}}{\partial x} + \frac{\partial \sigma_{xy}}{\partial y} + \frac{\partial \sigma_{xz}}{\partial z} \\
&= \lambda\frac{\partial \Delta}{\partial x} + \frac{2\mu\partial \varepsilon_{xx}}{\partial x} + \frac{\mu\partial \varepsilon_{xy}}{\partial y} + \frac{\mu\partial \varepsilon_{xz}}{\partial z} \\
&= \lambda\frac{\partial \Delta}{\partial x} + \mu\left\{\frac{\partial^2 u}{\partial x^2} + \left(\frac{\partial^2 v}{\partial x\partial y} + \frac{\partial^2 u}{\partial y^2}\right) + \left(\frac{\partial^2 w}{\partial x\partial z} + \frac{\partial^2 u}{\partial z^2}\right)\right\} \\
&= \lambda\frac{\partial \Delta}{\partial x} + \mu\nabla^2 u + \mu\frac{\partial}{\partial x}\left(\frac{\partial u}{\partial x} + \frac{\partial v}{\partial y} + \frac{\partial w}{\partial z}\right) \\
&= (\lambda + \mu)\frac{\partial \Delta}{\partial x} + \mu\nabla^2 u
\end{aligned} \tag{6}$$

Where, $\Delta^2 U$ = Laplacian of u:

$$\nabla^2 u = \frac{\partial^2 u}{\partial x^2} + \frac{\partial^2 u}{\partial y^2} + \frac{\partial^2 u}{\partial z^2}$$

By analogy we can write equations for v and w:

$$\rho\frac{\partial^2 v}{\partial t^2} = (\lambda + \mu)\frac{\partial \Delta}{\partial y} + \mu\nabla^2 v \tag{7}$$

$$\rho\frac{\partial^2 w}{\partial t^2} = (\lambda + \mu)\frac{\partial \Delta}{\partial z} + \mu\nabla^2 w \tag{8}$$

To obtain the wave equation, we differentiate these three equations with respect to x, y and z, respectively and add the results together. This gives:

$$\rho\frac{\partial^2}{\partial t^2}\left(\frac{\partial u}{\partial x} + \frac{\partial v}{\partial y} + \frac{\partial w}{\partial z}\right) = (\lambda + \mu)\left(\frac{\partial^2 \Delta}{\partial x^2} + \frac{\partial^2 \Delta}{\partial y^2} + \frac{\partial^2 \Delta}{\partial z^2}\right) + \mu\nabla^2\left(\frac{\partial u}{\partial x} + \frac{\partial v}{\partial y} + \frac{\partial w}{\partial z}\right)$$

That is:

$$\rho\frac{\partial^2 \Delta}{\partial t^2} = (\lambda + 2\mu)\nabla^2 \Delta$$

Or:

$$\left.\begin{aligned}
&\frac{1}{\alpha^2}\frac{\partial^2 \Delta}{\partial t^2} = \nabla^2 \Delta \\
&\text{where} \\
&\alpha^2 = \frac{\lambda + 2\mu}{\rho}
\end{aligned}\right\} \tag{9}$$

By subtracting the derivative of Eq. 7 with respect to z from the derivation of Eq. 5 with respect to y, we have that:

$$\rho\frac{\partial^2}{\partial t^2}\left(\frac{\partial w}{\partial y}-\frac{\partial v}{\partial z}\right)=\mu\nabla^2\left(\frac{\partial w}{\partial y}-\frac{\partial v}{\partial z}\right)$$

$$\left.\begin{aligned}\frac{1}{\beta^2}\frac{\partial^2\theta_z}{\partial t^2}&=\nabla^2\theta_z\\ \beta^2&=\frac{\mu}{\rho}\end{aligned}\right\} \tag{10}$$

By subtracting appropriate derivation we obtain similar results for oy and oz. These equation are different examples of the wave equation which we can write in the general form:

$$\frac{1}{V^2}\frac{\partial^2\psi}{\partial t^2}=\nabla^2\psi \tag{11}$$

where, V = Constant

For a plane wave solution, Let us consider the case where ψ is a function only of x and t so that Eq. 11 reduces to:

$$\frac{1}{V^2}\frac{\partial^2\psi}{\partial t^2}=\frac{\partial^2\psi}{\partial x^2} \tag{12}$$

Any function of (x-vt):

$$-\psi = f(x-vt) \tag{13}$$

This is a solution of Eq. 12 provided that ψ and its first two derivatives have no discontinuities. This solution known as D' Alembert's solution j, furnishes an infinite number of particular solution (e.g., $e^{k(x-vt)}$, Sin(x-vt) $(x-vt)^3$. Where we must exclude points at which these functions and their first two derivatives ceases to exists.

A wave is defined as a disturbance which travels through the medium. In our notation, the disturbance ψ is a volume change when:

$$\psi = \Delta \text{ and a rotation when } \psi = \theta_z$$

The velocity of a wave (illustration) for the Fig. 2, a certain part of the wave has reached the point P_0 at the time the coordinates of p_o is x_o, then the value of ψ at P_o is $\psi_o = F(x_o - vt_o)$ the same portion of the wave reaches P, at the time $t_o+\Delta t$, then we have the value of ψ at P_1 to be:

$$\psi_1 = f\{X_o+DX-V(t_0+\Delta t)\} \tag{14}$$

But since this is the same portion of the wave which was at P_o at time $t = t_0$, we have $\psi_o = \psi_1$:

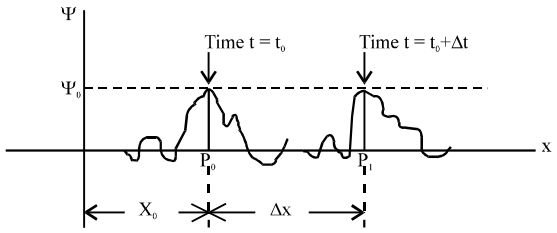

Fig. 2: Illustration of the velocity of a wave

$$X_0\text{-}Vt_0 = X_o\text{+}DX\text{-}V\ (t_0+\Delta t) \tag{15}$$

This quantity V is equal to $\Delta x/\Delta t$ and is the speed with which the disturbance travels:

$$\psi = f\ (x\text{-}Vt)+g(x+Vt) \tag{16}$$

represents two waves traveling along the x-axis in opposite direction of velocity V. Since the value of ø is independent of y and z, the disturbance must be everywhere in a plane perpendicular to the X-axis. This type of wave is known as the plane wave.

Considering a spherical wave solution, we have that the spherical wave is where the wavefronts have a series of concentric spherical surfaces. Let us express Eq. 11 in spherical coordinates (r, θ, ϕ), where θ = the colatitudes, ϕ = the longitude.

Therefore:

$$\frac{1}{V^2}\frac{\partial^2 P}{\partial t^2} = \frac{1}{r^2}\left\{\frac{\partial}{\partial r}\left(r^2\frac{\partial \psi}{\partial r}\right)+\frac{1}{\sin\theta}\frac{\partial}{\partial \theta}\left(\sin\theta\frac{\partial \psi}{\partial \theta}\right)+\frac{1}{\sin^2\theta}\frac{\partial^2 \psi}{\partial \varphi^2}\right\} \tag{17}$$

We consider only the spherical case where the wave motion is independent of θ and ϕ hence, is a function only of r and t. We therefore have by simplification that:

$$\frac{1}{V^2}\frac{\partial^2 \psi}{\partial t^2} = \frac{1}{r^2}\frac{\partial}{\partial r}\left(r^2\frac{\partial \psi}{\partial r}\right) \tag{18}$$

A solution of the above equation is:

- $\psi = 1/r\ f\ (r\text{-}Vt)$
- $\psi = 1/r\ g\ (r+Vt)$ is also a solution

The general solution of Eq. 18 is:

$$\psi = 1/r\ f\ (r\text{-}Vt)+1/r\ g\ (r+Vt) \tag{19}$$

In this equation, the first term represents a wave expanding outward from a central point and the second term represents a wave collapsing towards the central point. When r and t are fixed (r-Vt) is constant and hence, ψ is a constant. Thus at the instant t, the wave has the same value

at all points on the spherical surface of radius r. The spherical surfaces are wavefronts and the radii are rays. As the wave progresses outward from the centre, the radius increases by the amount V during each unit of time. The radius becomes very large and the portion of the wavefront near any particular point will be approximately plane. For a harmonic waves, now having looked at the geometrical aspects of waves, that is, the way in which the wave depends upon the space coordinate, therefore ø is a function of t also, we can also consider the time dependence of waves. Harmonic waves are the simplest form of time variation. It is a wave involving sine or cosine expression such as:

$$\Psi = A \cos 2\pi K(x-Vt) \tag{20}$$

$$\Psi = A \sin 2\pi K (Lx+my+nz-Vt) \tag{21}$$

$$\Psi = {}^{B}/_{r} \cos 2\pi K (r+Vt) \tag{22}$$

For a fixed point, ψ varies as the sine or cosine of the time: hence the motion is simple harmonic. The values of ø range from +A to -A for the plane wave of Eq. 20 and 21 and from +B/r for the spherical wave of Eq. 23. The limiting value, A or B/r, is known as the amplitude of the wave ψ. For a fixed value of t, whenever x in Eq. 20 increases by the amount i/k, the argument of the cosine increases by 2π and hence the value of y repeats. The quantity k => wave number.

In Eq. 21 and 22 (lx+my+nz) and r represent the distance the wave traveled from the origin, hence are equivalent to x in Eq. 20. In the space coordinates in Eq. 20-22 are kept fixed and t allowed to increase the value of ψ repeats each time that t increases by the amount:

$$KVT = 1 = {}^{VT}/_{\lambda}$$

Consequently $T = {}^{\lambda}/_{V,}\ v = {}^{1}/_{T} = {}^{V}/_{\lambda}$, $V = v\lambda$:

T = Period
V = Frequency of wave
ω = 2
V = 2πKV = angular frequency

Equation 4 can be written in the following equivalent forms:

$$\Psi = A \cos 2\pi K (x-Vt) = A \cos {}^{2\pi}/_{\lambda} (x-Vt)$$
$$= A \cos(2\pi Kx-\omega t) = A \cos\omega({}^{x}/_{V}-t)$$
$$= A \cos 2\pi({}^{x}/_{\lambda}-Vt) = A \cos 2\pi (Kx-Vt)$$

Let us consider P-waves and S-waves. So far, we have merely inferred that y is some disturbance which is propagated from one point to another with the speed V. However, in a homogeneous isotropic medium, Eq. 9 and 10 must be satisfied. We can identify the functions Δ and θ_x with ψ and conclude that two types of waves can be propagated in a homogeneous isotropic medium, one corresponding to changes in the dilatation, Δ, the other to changes in one or more component of the rotation given as follows:

$$\theta_x = \partial w/\partial y - \partial v/\partial z \tag{23a}$$

$$\theta_y = \partial u/\partial z - \partial w/\partial x \tag{23b}$$

$$\theta_z = \partial v/\partial x - \partial u/\partial y \tag{23c}$$

The first type is variously known as a dilatational, longitudinal, irrotational, compressional or P-waves, the latter name being due to the fact that this type is usually the first (primary) event on an earthquake recording. The second type is referred to as the shear, transverse, rotational or s-wave (it is usually the second event observed on earthquake records). The p-wave has the velocity $\propto$ in Eq. 9 and the s-wave has the velocity β in Eq. 10 where:

$$\left.\begin{aligned}\alpha &= \left\{\frac{\lambda+2\mu}{\rho}\right\}^{\frac{1}{2}}\\ \beta &= \left(\frac{\mu}{\rho}\right)^{\frac{1}{2}}\end{aligned}\right\} \tag{24}$$

Since the elastic constants are positive, α is always greater than β, if; $\mu = \beta/\alpha$.
we have that:

$$\gamma^2 = \frac{\beta^2}{\alpha^2} = \frac{\mu}{\lambda+2\mu} = \frac{\frac{1}{2}-\sigma}{1-\sigma} \tag{25}$$

Recall that:

$$\sigma = \frac{\lambda}{2(\lambda+\mu)} \tag{26}$$

From Eq. 26, as σ decreases from ½ to zero. γ increases from zero to its maximum value, $1/\sqrt{2}$ thus, the velocity of the S-wave ranges from zero up to 70% of the velocity of the p-wave. For fluid μ is zero and hence, β and γ are also zero. Therefore, S-wave does not propagate through fluids.

Let us investigate the nature of the motion of the medium corresponding to the two types of wave motion. Consider a spherical p-wave of the type given by Eq. 22. The Fig. 3 shows wavefronts drawn at quarter wavelength intervals, t being chosen so that KVt is an integer. The arrows represent the direction of motion of the medium at the wavefront.

The medium is undergoing maximum compression at B (that is, the dilatation Δ is a minimum) and minimum compression (maximum Δ) at the wavefront D. we can picture the plane-wave situation by imaging that the radius in the Fig. 3 has become very large so that the wavefront are practically plane surfaces. The displacement will everywhere be perpendicular to these planes so that there will no longer be convergence or divergence of the particles of the medium as the move back and forth parallel to the direction of propagation of the wave. Such a displacement is longitudinal which explains why P-waves are sometimes called longitudinal waves. P-waves are

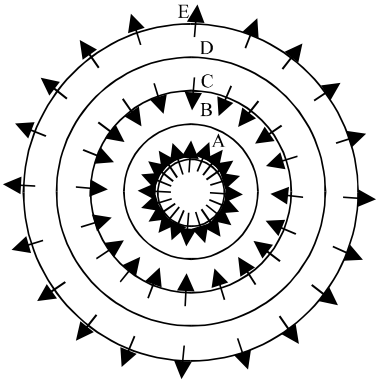

Fig. 3: Displacement for a spherical P-Wave

the dominant waves involved in seismic exploration. Now, to determine the motion of a medium during the passage of an S-wave, we recall Eq. 10 and then consider the case where a rotation θz which is a function of x and t only is being propagation along the x-axis. We have that:

$$\frac{1}{\beta} = \frac{\partial^2 \theta_Z}{\partial t^2} = \frac{\partial^2 \theta_Z}{\partial x^2}$$

Since:

$$\theta_z = \frac{\partial v}{\partial x} - \frac{\partial u}{\partial y} = \frac{\partial v}{\partial x}$$

From Eq. 23 it is clear that the wave motion consists solely of a displacements V of the medium in the y-direction. V being a function of both x and t. since v is independent of y and z, the motion is everywhere the same in a plane perpendicular to the x-axis therefore this case is that of a plane s-wave traveling along the x-axis. From Eq. 16, the displacement v must have the form:

$$V = f(x-\beta t)+g(x+\beta t) \tag{27}$$

From the Fig. 4 (motion during passage of an S-wave), we can visualize the above relation. When the wave arrives at P, it causes the medium in the vicinity of p to rotate about the axis Z^1Z^{11} (parallel to the Z-axis) through an angle ε. Since its infinitesimal strains, ε must be infinitesimal and we can ignore the curvature of the displacements and consider that points such as p^1 and p^{11} are displaced parallel to the y-axis to the points Q^1 and Q^{11}. Therefore, as the wave travels along the x-axis the medium is displaced transversely to the direction of propagation. Since the rotation varies from point to point at any given instant the medium is subjected to varying shearing stresses as the wave move along and this accounts for the name shear wave. In practice S-wave motion is usually resolved into components parallel and perpendicular to the surface of the ground; these are known respectively as SH and SV waves. When the wave is traveling neither horizontally nor vertically, the motion is resolved into a horizontal (SH) component in the vertical plane through the direction of propagation. Shear wave have two degrees of freedom, unlike p-waves which have only one-along the radial direction. Since the two degrees of freedom of

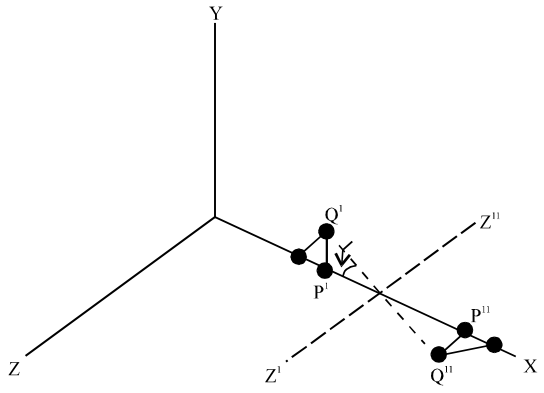

Fig. 4: Motion during passage of an S-wave

S-waves are independent, we can have an S-wave which involves motion in only one plane, e.g., SH or SV motion have the same frequency and a fixed phase difference; such a wave is elliptically polarized. Polarization of S-wave is not important in Seismic exploration. For a medium which is not homogeneous and isotropic, it may not be possible to resolve wave motion into separate p-wave and s-wave but is valid for practical purposes.

MATERIALS AND METHODS

The instruments adopted for this investigation include: cables, compass clinometers, D.C battery, geophones, GPS, hammer, plate and seismograph. The instruments were then connected to the seismograph which record the signals picked up by the array of geophones after energy has been detonated through the weight drop using the hammer and plate. The battery serves as energy source to the seismograph itself. The geophone array on a whole is 24 channels and it is laid out in a split spread manner and such that one of its ends is connected to the battery while the other end is connected to the hammer through the cable. After setting up appropriately, then the seismograph is switched on after which it is armed, before shots were taken through the hammer against the plate to release energy for the forward, reverse and intermediate shooting. The records were adequately taken and saved on the seismograph for accessibility when processing and interpretation time comes. This was done severally to obtain a whole lot of data for different offsets namely 2, 4, 6 m, 8/9,12/13 etc. Shots were taken for 22 different profiles. The GPS and the compass were used to know the elevations and the bearing of the location under observation with respect to the north, respectively.

The data obtained was analyzed by picking the first arrivals using the Seismic Imager computer software. Adopting the use of the Pickwin as part of the software, signals were plotted with shot distances against arrival times using a geophone offset of 4 m. A 22 profile plot which consist of the forward, reverse and intermediate were obtained. Then the first arrival times were picked before saving the first arrivals such that we can then apply the saved results to obtain our seismic refraction plot using the Plotrefrac as shown in Fig. 5a and b for profiles 1 and 2, while the remaining profiles 3-22 were also done. Then the depth model was generated using the tomography as represented in Fig. 6a and b for profiles 1 and 2 and depth model for profiles 3-22 were also done, such that velocity estimates were obtained to the top of the third (3rd) layer in order to have a near accurate seismic section. Invariably, the fourth (4th) layer would not have been accurately described, hence not treated in details, since our zone of interest really lies above this layer.

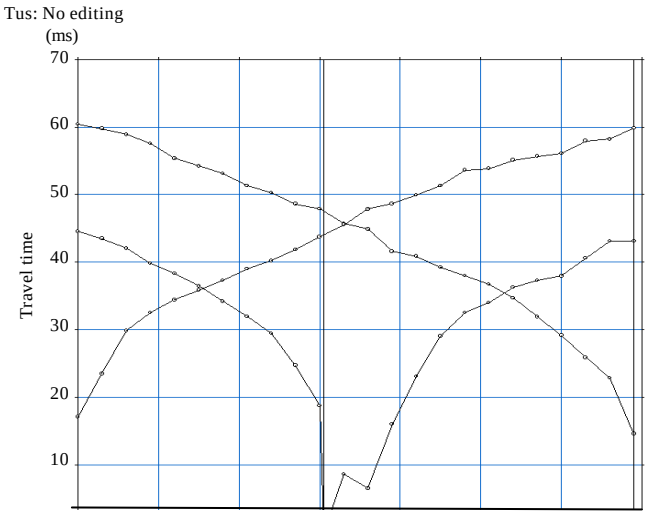

Fig. 5a: Seismic plot for profile 1

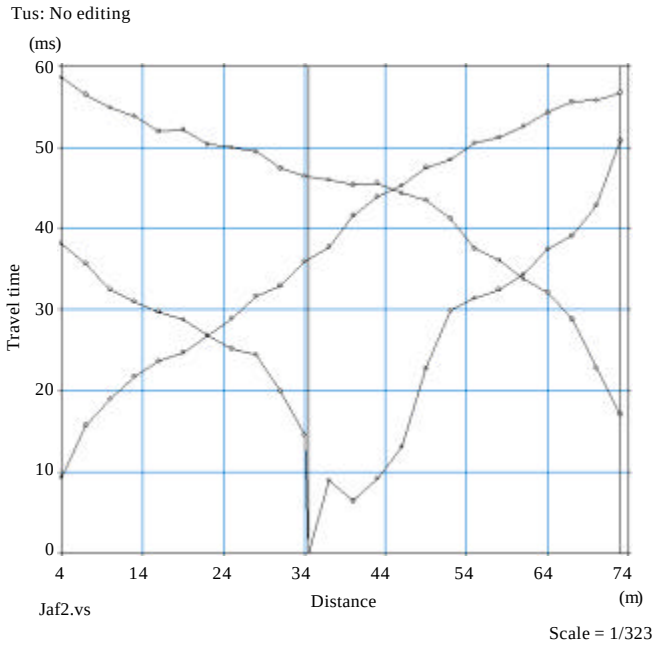

Fig. 5b: Seismic plot for profile 2

Numeric results obtained from all these are presented in Table 1. From the seismic data, the velocities of sound were determined in the first, second, third and fourth layer.

RESULTS AND DISCUSSION

From the data, velocities of sound were determined for the first, second, third and fourth layer. Therefore the velocity of sound in the first layer for profiles 1-22 is determined on the basis of an

Table 1: Results for seismic data showing velocities and thickness

	Velocity (m sec^{-1})				Thickness (m)			
Profiles	Layer 1	Layer 2	Layer 3	Layer 4	Layer 1	Layer 2	Layer 3	Layer 4
1	600	1000	2000	-	2	5	7	-
2	600	1100	1500	2500	4	3	7	10
3	600	1300	2500	-	5	8	12	-
4	600	1100	1700	2500	3	3	6	12
5	900	1600	2500	-	6	7	11	-
6	600	1500	2600	-	4	8	10	-
7	900	1700	2600	-	6	7	10	-
8	600	1600	2500	-	4	7	9	-
9	700	1700	2500	-	5	7	9	-
10	600	1000	1600	2500	4	3	7	8
11	800	1700	2700	-	6	7	8	-
12	800	1600	2700	-	5	6	7	-
13	900	1700	2300	-	5	4	8	-
14	900	1800	2500	-	6	6	10	-
15	900	1800	2400	-	6	7	9	-
16	600	900	1700	2500	2	3	5	8
17	800	1700	2500	-	5	6	8	-
18	800	1800	2400	-	6	6	9	-
19	800	1500	2400	-	4	6	9	-
20	500	900	1600	2500	2	3	5	9
21	900	1700	2300	-	6	4	9	-
22	800	1600	2500	-	5	7	9	-

average velocity of sound in layer 1 as 736 m sec^{-1} and average thickness of 4.5 m. However, for layer 2 the velocity of sound for profiles 1-22 (Table 1), we have the average velocity of sound to be 1468.18 m sec^{-1} and corresponding thickness of 5.59 m.

The same procedure applies to layer 3 to give us an average velocity of sound of 2272.73 m sec^{-1} and corresponding thickness of 8.36 m. The average velocity of sound derived from layer 4 is 2500 m sec^{-1} and corresponding thickness of 2.14 m. Therefore, the average velocities of sound in layers 1, 2, 3 and 4 are 736, 1468.18, 2272.73 and 2500 m sec^{-1}, respectively.

Layered models obtained mainly signifies three layers for the study area, with layer 1 having very low velocities of sound, layer 2 having and intermediate velocities of sound while layer 3 has the highest velocities of sound at about 2600 m sec^{-1}. these are evident in Fig. 6a and b shown below. From the layered model derived from the seismic results, all the profiles of the study have three layers delineated. Hence, for profile 1-4 (Fig. 7a). Sand is in layer 3 and it falls within a depth of 10-22 m and a maximum velocity of sound of 2800 m sec^{-1}. For profile 5-16 (Fig. 7b), sand lies between a depth of 7-22 m, while for profile 17-19 (Fig. 7c) the layer of sand lies a little above the 5 m mark and extends to about 12 m depth with a maximum velocity of sound of 2300 m sec^{-1}. Finally, profiles 20-22 (Fig. 7d) indicate that the depth of sand ranges between 11-23 m with a maximum velocity of sand of 2700 m sec^{-1}.

Therefore, we deduced that layer 1 has an average velocity of 736 m sec^{-1} indicating loose soil type with organic matter content, this being the top soil whose thickness falls between 2 and 6 m. On the other hand, layer 2 has an average velocity of 1468.18 m sec^{-1}, we can then infer that this layer is made up of wet clay (lateritic clay). The thickness of this layer ranges from 3 to 8 m.

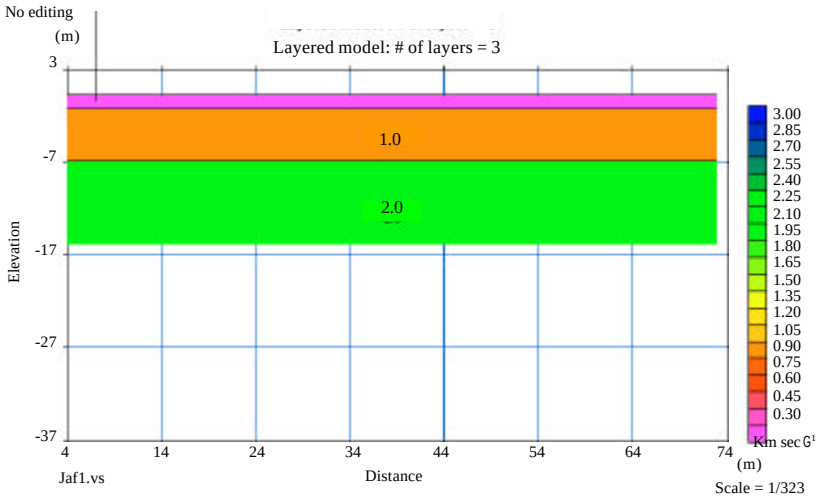

Fig. 6a: Depth Model Showing Different Layers obtained from seismic profile 1

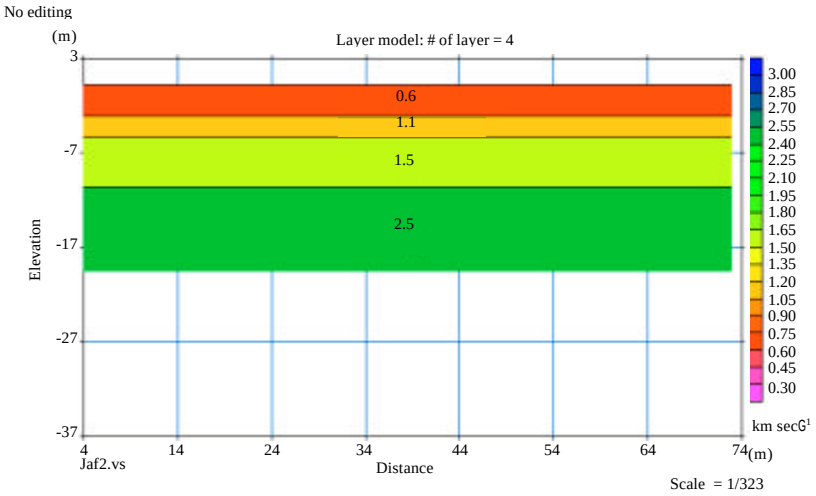

Fig. 6b: Depth Model Showing Different Layers obtained from seismic profile 2

Furthermore, layer 3 can be said to be associated with an average velocity of 2272.73 m sec^{-1} (Fig. 7) which indicates a mixture of sand, silt, gravel and alluvium, hence, we can say it is a combination of sand and compacted clay, although we have more of sand here. The thickness of this layer from seismic sections of Fig. 7 showed that we have values ranging from 5 to 12 m. This then reflects that the third layer being more of sand has good capillary action, hence, a good source of ground water. It is clearly evident from Fig. 7 based on the synclinal structures derived that there are good unconfined aquifers within the third layer which will definitely yield good potable ground water. Also, this layer has the tendency of harboring high yield aquifer thus it allows the free movement of water which can be tapped for human and animal consumption.

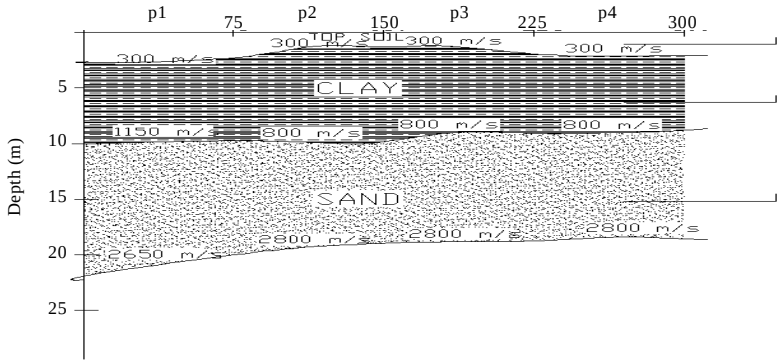

Fig. 7a: Seismic section DD' for profiles 1-4

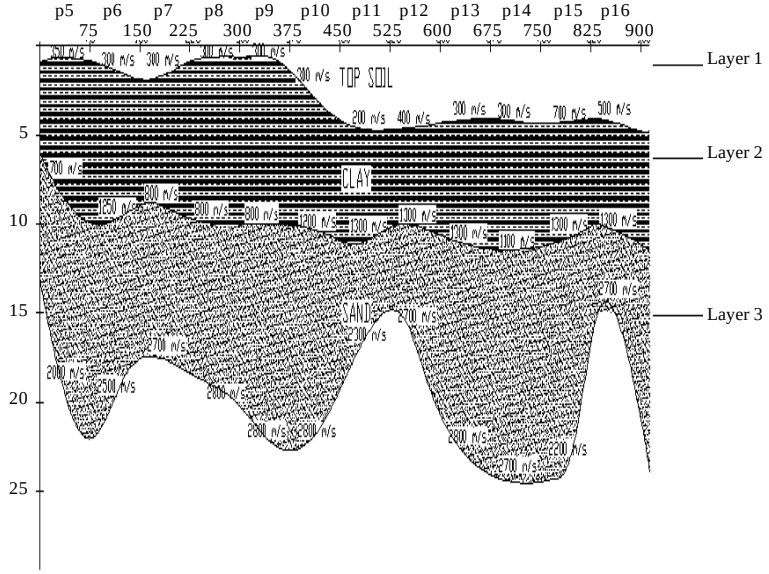

Fig. 7b: Seismic section EE' for profiles 5-16

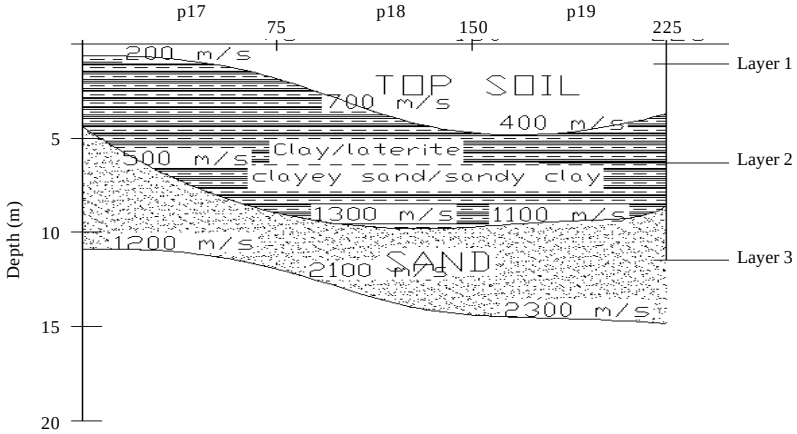

Fig. 7c: Seismic section FF' for profiles 17-19

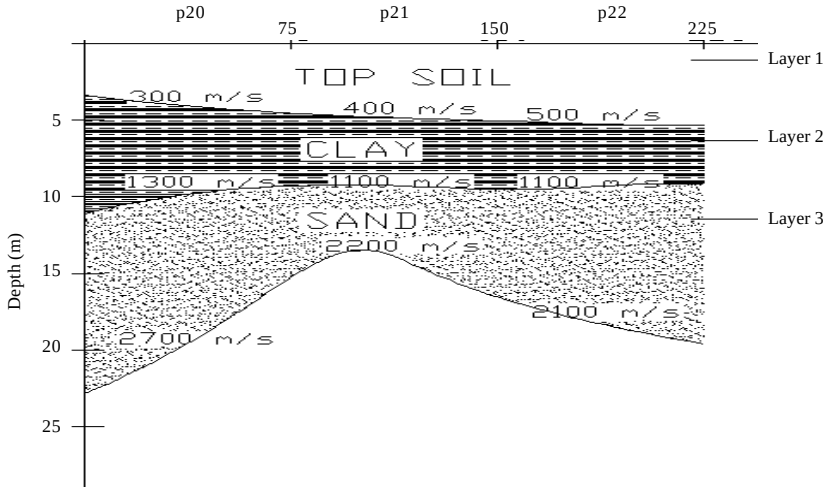

Fig. 7d: Seismic section GG' for profiles 20-22

CONCLUSION

The study carried out in the area showed that there is a good quality water resource which is pollution free, with deep aquifer having a tendency of high productivity, due to the presence of sand and clay. It can also be said that sand being pervious is a good aquifer and clay serves as a seal for the sand since it tends to undergo compaction by overburden pressure. On the other hand, sand also possesses a good capillary action which is also a good attribute of an aquifer with a high productivity.

When a borehole is sunk to a depth of about 100 m therefore, the area is generally a good site for location of borehole with high tendency for good water supply. This was confirmed by the seismic results gotten which clearly shows the position of each layer, hence giving us precisely where the aquifer lies although it was only able to achieve this for the first aquifer unit because the energy source used was minimal hence not strong enough to image deeper horizons.

It is therefore suggested that boreholes should be sunk within the study area since it has a high yield aquifer. This study also gives room for further studies in this area to determine the recharge capacity of the aquifer(s) and production rate. Then the cone of depression around the water table can also be researched into to further consolidate this study. Adequate measures can also be put in place not to create septic tanks at close proximity with regions marked for ground water production to avoid pollution. Also to delineate lower substratum, stronger energy source must be used.

REFERENCES

Ackermann, H.D., L.W. Pankrate and D. Danserean, 1986. Resolution of ambiguities of seismic refraction travel time curves. Geophysics, 51: 223-235.

Adegoke, S.O., T.F.J. Dessauvagie and A.J. Whiteman, 1970. Macrofauna of ewekoro formation (Paleocene) of Southwest Nigeria. Proceedings of the Conference on African Geology, December 7-14, 1970, University of Ibadan, Nigeria, pp: 269-276.

Birch, F., 1966. Compressibility Electric Constant. In: Handbook of Physical Constants, Clark, S.P. (Ed.). Geological Society of America, USA., pp: 97-173.

Haeni, F.P., 1986. Application of seismic refraction methods in groundwater modeling studies in New England. Geophysics, 51: 236-249.

Hunter, J.A. and S.E. Pullan, 1990. A vertical array method for shallow seismic refraction survey of the seafloor. Geophysics, 55: 92-96.

Kogbe, C.A., 1989. Geology of Nigeria. 2nd Edn., Rockview Nigeria Ltd., Jos, Nigeria, Pages: 538.

Lennox, D.H. and V. Carlson, 1967. Geophysical exploration for buried valleys in an Area North of two hills, Alberta. Geophysics, 32: 331-362.

Ogbe, F.A.G., 1970. Stratigraphy of Strata Exposed in Ewekoro Quarry Western Nigeria. In: Africa Geology, Dessauvage, T.F.J. and A.J. Whiteman (Eds.). University of Ibadan Press, Nigeria, pp: 305-324.

Philip, A.O., 2001. An Introduction to Geophysical Exploration. McGraw-Hill, New York.

Slansky, M., 1962. Contribution to the geological study of coastal sedimentary basin of Dahomey and Togo Bur. Rech. Geol. Min. Mem., 11: 270-270.

Tearpock, D.J. and R.E. Bischke, 1991. Applied Subsurface Geological Mapping. Prentice-Hall PTR Press, Englewood Cliffs, NJ., USA., pp: 94-96.

Van Overmeeren, R.A., 1981. A combination of electrical resistivity, seismic refraction and gravity measurements for ground water exploration in Sudan. Geophysics, 46: 1304-1313.

Watts, R.D., A.W. England, R.S. Vickers and M.F. Meier, 1975. Radio-echo sounding on south cascade glacier, Washington, using a long-wavelength, mono-pulse source. J. Glaciol., 15: 459-461.